11^{th} International Conference on Fracture Mechanics of Concrete and Concrete Structures
FraMCoS-11
J. M. Chandra Kishen, A. Ramaswamy, S. Ray and R. Vidyasagar (Eds)
https://doi.org/10.21012/FC11.092345

q-STATISTICS FOR INTER-EVENT TIME DISTRIBUTION OF ACOUSTIC EMISSION IN CONCRETE FRACTURE UNDER MONOTONIC LOADING

Nitin B. Burud *, **J. M. Chandra Kishen** †

*University of Surrey
Guildford, United Kingdom
e-mail: nitinburud@gmail.com

†Indian Institute of Science
Bangalore, India
e-mail: chandrak@iisc.ac.in

Key words: Concrete Fracture, Acoustic Emission, Inter-event time distribution, Tsallis Entropy, q-statistic

Abstract. The present work extends non-extensive statistical formulation to the inter-event time distribution of acoustic emission (AE) events generated by the fracture process in plain concrete. The time interval between two consecutive events can be defined as inter-event time and the distribution of inter-event time is pivotal for understanding the underlying event-generating process. The magnitude and inter-event time of AE events may be correlated, resulting in repeated intervals of clustered AE activity and quiescence often observed in the concrete fracture process. The crack size is considered to be correlated with AE wave magnitude (amplitude) therefore, the long-tailed magnitude distribution is usually used to infer the extent of cracking. Similarly, the inter-event time distribution can be used as an indicator of the frequency or rate of occurring events. The AE phenomena resulting from the fracture process exhibit non-Poissonian behavior, meaning that the time intervals between AE events are not independent and identically distributed. AE inter-event time distribution in concrete has not been explored as much as magnitude distribution however, few studies including rock fracture, concrete under compression, and seismology reported long-tailed behavior of the inter-event time distribution often modeled by power-law, log-normal, Weibull, Gamma as well as q-statistical exponential distributions. Recently, Burud and Chandra Kishen proposed two q-statistical distribution functions based on exponential and power law ansatzes. The power law ansatz-based distribution function is shown to better represent AE magnitude distribution in concrete. We explore the exponential ansatz-based distribution function to inspect AE inter-event time distribution. The variation of q-statistical parameters for AE inter-event time distribution with respect to specimen size is discussed in detail.

1 INTRODUCTION

Crack size and crack growth rate are fundamental aspects of fracture mechanics concerning the behavior of cracks in materials. Crack size refers to the physical dimensions or length of a crack in material while crack growth rate refers to the rate at which the crack size increases as the material undergoes applied stress. Both these aspects are relatively easier to comprehend in the presence of a single crack propagating through material, conversely, it becomes a daunting task in the presence of multiple or clusters of cracks. The fracture process in

concrete like heterogeneous materials is well known for its multi-scale and multi-mechanistic behavior characterized by a fracture process zone ahead of the crack tip. Nowadays, acoustic emission monitoring has become an excellent tool to observe such complex fracture processes in materials. The AE monitoring relies on acquiring stress waves emitted by the sudden release of strain energy due to cracking in materials through piezoelectric sensors. Each crack generates an omnidirectional stress wave and, if it is large enough and above some threshold level, it can be detected by multiple sensors. Such detection of the AE waveform by multiple sensors is recognized as an AE event which can be further analyzed to determine the location of the crack. Many studies have elaborated on the correlation between crack size and amplitude/energy of acoustic emission waves and derived useful parameters to evaluate the damage state in materials [1–3]. Such studies involve statistical tools accounting for multi-scale cracking phenomena resulting in damage state estimation based on crack size. However, not only crack size but the occurrence of cracks over the time scale can also be explored through acoustic emission monitoring. The arrival of a stress wave at the AE sensor location can be regarded as an approximate crack occurrence time. When several such cracks occur successively, the time interval between cracks can be considered as interevent time or interarrival time. The interevent time is a random variable and can be used to understand the temporal patterns and dynamics of the transient fracture process. Particularly in seismology, interevent times are deeply studied to understand insights into earthquake occurrence mechanisms, the clustering in seismic events, and the probability of future earthquakes.

The exponential distribution is commonly used to model waiting times in various real-world systems having memoryless property signifying the probability of future events does not depend on past events. The exponential distribution represents those Poissonian processes that exhibit random and independent events. Contrarily, many real-world systems such as earthquakes, internet traffic, financial market volatility, etc exhibit long-tailed behavior caused by non-Poissonian processes, and are often described by Gamma, Weibull, lognormal and other long-tailed distributions. The non-Poisonian processes do not exhibit a constant rate of event occurrence mainly caused by the clustering of events, memory effects, and long-range correlations.

Although fracture mechanics of concrete has been well studied at a macroscopic scale providing some insightful laws and mathematical models, the physical description of micromechanics is still under investigation and not yet well understood. Acoustic emission observed during the fracture process mainly contributes to the understanding of concrete micromechanics considering abundant studies in the literature. In the present work, we seek palliative treatment based on entropy formulation for the problem of modeling inter-event time distribution rather than approaching it from the first principles of physics. Such an approach has been proven effective in seismology where collective properties of earthquakes have been reproduced in statistical models [4, 5]. Therefore, there is a hope to discover consistent statistical patterns and trends in the AE data which can be useful for understanding fracture process and structural health monitoring applications.

2 MOTIVATION

Seismic events in geology and as well as acoustic emission events in material fracture have striking similarities. Earthquakes are mainly divided into main shocks, foreshocks, and aftershocks based on their temporal and spatial relationship to one another. The main shock is the largest and most significant earthquake in the sequence. The preceding and succeeding earthquakes to the main shock are the foreshocks and aftershocks respectively. Although foreshocks can provide valuable insights into the processes leading up to a main shock, they are not a necessary precursor for every significant earthquake. On the other hand, after-

shocks are a common occurrence after a significant earthquake and are an integral part of the seismic sequence. Due to the abundance of aftershock earthquakes, extensive studies on aftershocks are available in the seismology literature compared to foreshocks which led to several empirical and statistical models for describing the inter-event time distribution of earthquakes. In 1894, Omori [6] proposed an empirical Equation 1a known as Omori's law stating the rate of aftershocks decreases over time following a power-law decay . Utsu [7] modified version of Omori's law in 1961 expressed in Equation 1b where *t* is the time after the large event, k and c are the productivity (depending on the magnitude of the main shock) and case-dependent time scale parameters respectively. The parameter *p* in Equation 1b is considered as a universal exponent $p \approx 1$.

$$n(t) = \frac{k}{c+t} \tag{1a}$$

$$n(t) = \frac{k}{(c+t)^p} \tag{1b}$$

There is a common consensus in seismology, that earthquakes follow Omori's law on short time scales while on long time scales earthquakes exhibit exponential behavior for waiting time distribution possibly due to the independence of earthquake events over the long time scales. Therefore, the Gamma distribution proposed by Corral [8] became pivotal at an intermediate time scale due to its validity over many different geographic regions. However, the Gamma distribution assumes a memoryless process with stationarity which again questions its validity.

Unlike seismic activity, primarily triggered by stress redistribution along the tectonic plates following a large earthquake, acoustic emission in the material fracture is influenced by local stress concentrations and crack interactions within the material. The processes governing acoustic emission are complex and involve multiple micro-cracks and interactions between them. Moreover, the time scale of acoustic emission events and earthquakes is vastly different. Therefore, there is a need for a different approach that can describe AE inter-event time statistics.

A recent approach based on Tsallis entropy [4] provides a generalized perspective on earthquake statistics. The non-extensive statistical mechanics (NESM) based on the Tsallis entropy has been successfully applied to study the collective properties of earthquake [5] which includes frequency-magnitude distribution as well as spatio-temporal (inter-event time and distance) distribution. A similar approach was initiated to study acoustic emission in the material fracture as well [9–11]. Saltas *et al.* [9] concluded the suitability of NESM for brittle rocks under monotonic uniaxial compression using the q-exponential function. Greco *et al.* [10] also used the q-exponential function to describe inter-event time distribution for concrete and basalt under compression. Burud and Chandra Kishen [11] explored the frequency-magnitude relationship through NESM formulation and proposed two q-deformed distributions based on power law and exponential ansatzes. The present work extends the application of NESM to inter-event time distribution observed in concrete fracture. Section 3 briefly explains Tsallis entropy and exponential ansatz-based NESM formulation for the inter-event time distribution. The experimental setup is briefly explained in Section 4. The inter-event time distribution and resulting q-statistical parameters obtained from experimental data are illustrated in Section 5 followed by the discussion on the physical meaning of the q-statistical parameters in Section 6.

3 NON-EXTENSIVE STATISTICAL MECHANICS

Consider a one-dimensional random variable *X* with probability density function *p(x)*. The Tsallis entropy S_q for *x* is given as:

$$S_{q\neq 1} = k_B \frac{1 - \int_0^\infty \mathrm{p}^q(x)\,\mathrm{d}x}{q-1} \tag{2}$$

where q is known as the entropic index and k_B is the Boltzmann constant. We assume $k_B = 1$. The Boltzmann constant is a conversion factor to link the average kinetic energy of particles with the thermodynamic temperature of the gas which is not relevant in the present study. The maximization of the Tsallis entropy subjected to some constraints results in a distribution function proposed by Silva *et al.* [12] expressed in Equation 3.

$$p(x) = \left[1 - \frac{(1-q)}{(2-q)}(x - \bar{x}_q)\right]^{\frac{1}{(1-q)}} \tag{3}$$

where $\bar{x}$ is escort normalized mean expressed as $\bar{x}_q = \int_0^\infty x\pi_q(x)dx$ and $\pi_q(x)$ is escort probability given as by,

$$\pi_q(x) = \frac{p^q(x)}{\int_0^\infty p^q(x)dx} \tag{4}$$

To obtain the NESM formulation for representing inter-event time distribution, we substitute Equation 5 in Equation 3 and obtain cumulative probability distribution function proposed by Burud and Chandra Kishen [11] (where detailed derivation and description is available) as expressed in Equation 6.

$$x - \bar{x}_q = \alpha_\tau 10^{\beta_\tau \xi} \tag{5}$$

$$P(T \geq \xi) = \left[1 - \frac{(1-q_\tau)}{(2-q_\tau)}\alpha_\tau 10^{\beta_\tau \xi}\right]^{\frac{(2-q_\tau)}{(1-q_\tau)}} \tag{6}$$

$$q_\tau \to 1 \quad P(T \geq \xi) = e^{-\alpha_\tau 10^{\beta_\tau \xi}} \tag{7a}$$

$$q_\tau \to 1.5 \quad P(T \geq \xi) = \frac{1}{1 + \alpha_\tau 10^{\beta_\tau \xi}} \tag{7b}$$

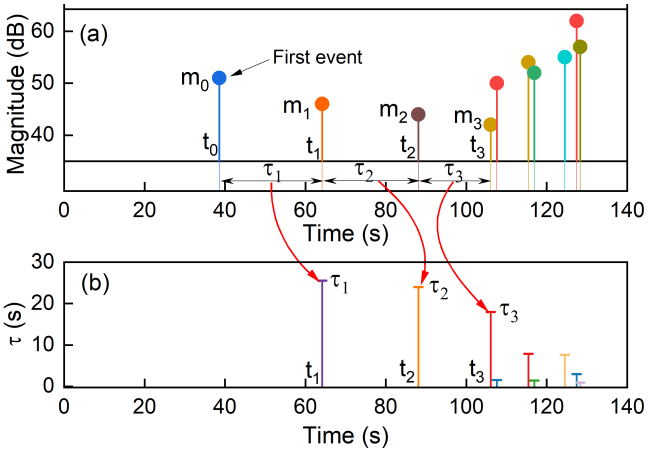

Figure 1: a) First few Acoustic emission events over the time scale and, b) inter-event time. m_i,t_i, and τ_i are the magnitude, arrival time, and inter-event time of the *ith* event.

The parameters of the distribution function (Equation 6) can be determined by fitting it over experimentally observed inter-event time. Although the parameters are defined for variable ξ, we add subscript τ indicating the inter-event time which will be later useful to compare results of the present work to the q-statistical parameters for AE magnitude distribution from [11]. The entropic index q_τ quantifies the long-tailed behavior of the distribution which ranges from 1 to 2. Equation 6 results in Equations 7a and 7b in the limit, $q_\tau \to 1$ and $q_\tau \to 1.5$ respectively. The inter-event time needs to be scaled logarithmically as $\xi = log_{10}\tau$. For simplicity (avoiding rules of change of variable), if $\xi = log_{10}\tau$ is substituted in Equations 7a and 7b results in $P(T \geq \tau) \propto e^{-\alpha_\tau \tau^{\beta_\tau}}$ and $P(T \geq \tau) \propto \frac{1}{1+\alpha_\tau \tau^{\beta_\tau}}$ respectively. The former expression is a stretched exponential and becomes exponential distribution $\beta_\tau = 1$ exhibiting exponential tail. The latter expression represents power law-like distribution signifying long-tailed distribution. The parameters α_τ and β_τ are the location and scale parameters of the distribution. The location parameter gives an idea of the central tendency of the distribution while the scale parameter controls the stretch or shape of the distribution.

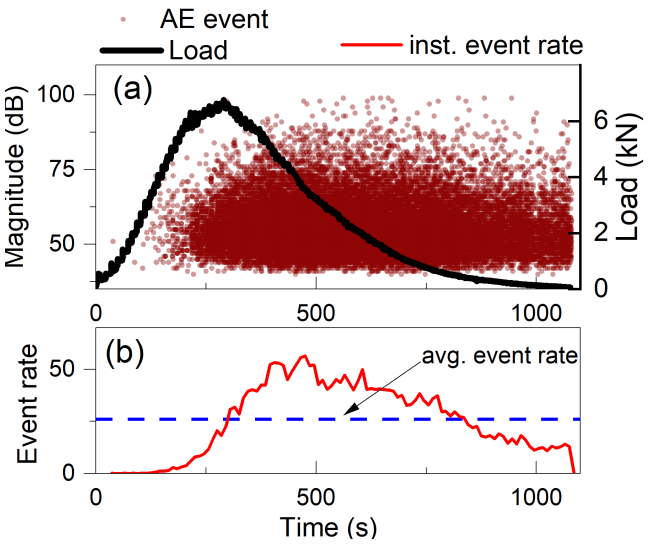

Figure 2: a) Loading history and acoustic emission events over the test duration in a large beam (B2), b) Average vs. instantaneous event rate.

4 EXPERIMENTAL SETUP

To study the AE inter-event time distribution, plain concrete notched beams of three different sizes were tested under three-point bending consisting of three specimens for each beam size as shown in Table 1. For maintaining monotonically increasing quasi-static loading, the crack propagation rate was controlled using crack mouth opening displacement (CMOD/clip gauge) at 1 μm/s. Six resonant-type piezo-electric acoustic emission sensors R6D of Physical Acoustic Corporation were attached to the beam surface at specific locations for the acquisition of acoustic emissions. Readers are advised to refer [11] for a detailed description of the experimental setup, AE sensor position, and load-deformation curves.

Table 1: Details of beam dimensions

Designation	Depth (mm)	Width (mm)	Span (mm)	Notch (mm)
Small	75	50	337.5	15
Medium	150	50	675	30
Large	300	50	1350	60

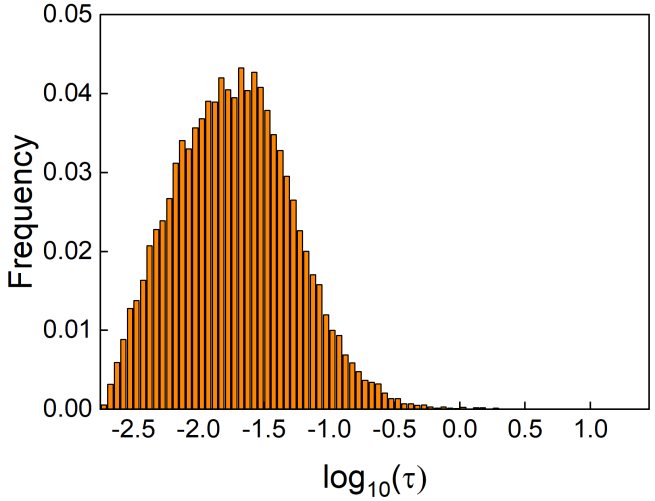

Figure 3: Probability distribution of inter-event time for a large beam (B2).

5 RESULTS

5.1 INTER-EVENT TIME

The applied load, controlled by crack mouth opening displacement, allowed stable crack growth in the beam specimens. Although the loading rate is constant, the micro-cracks occurring at the crack tip in concrete-like heterogeneous material is a spatio-temporal stochastic process. The instance of every crack occurrence releases strain energy which travels through the material as an omnidirectional stress wave. The stress wave acquired by an AE sensor is known as *hit* and if the same wave is acquired by multiple sensors then it is counted as an AE event according to the definition. The arrival time of the stress wave at the first sensor and its amplitude in dB is considered as the occurrence time and magnitude of the event. Consequently, every AE event acquired during the test can be represented as a pair of random variables (m_i, t_i) for $i = 0, 1, 2, ...N-1$, where m_i and t_i represent magnitude and arrival time of the *ith* event respectively. Figure 1 shows the first ten AE events acquired during one of the specimens. The occurrence of the first AE event is considered as initiation of the AE activity. The inter-event time of the consecutive events can be determined as $\tau_i = t_i - t_{i-1}$ for $i = 1, 2, ...N$, where N is the total number of AE events. Descriptive statistics of the inter-event time (on a

Table 2: Statistics of inter-event time distribution

Beam	No.	Size (mm)	# events	Min. (s)	Max. (s)	Mean (s)	Std. dev (s)	M.A.D. (s)	Test Time (s)
Small	B1	75	9008	0.0021	8.7	0.091	0.221	0.083	820.1026
	B2	75	1388	0.0042	51.4	0.621	1.931	0.649	861.4187
	B3	75	10651	0.0022	34.3	0.096	0.438	0.092	1023.657
Medium	B1	150	7956	0.0018	9.4	0.140	0.322	0.142	1117.481
	B2	150	19142	0.0019	17.5	0.072	0.342	0.078	1380.382
	B3	150	16446	0.0019	21.7	0.077	0.314	0.076	1267.03
Large	B1	300	26664	0.0019	33.7	0.035	0.245	0.031	931.4919
	B2	300	27169	0.0018	25.6	0.038	0.263	0.035	1041.804
	B3	300	34166	0.0018	12.4	0.038	0.179	0.034	1286.938

Min.- Minimum, Max. - Maximum, M.A.D. - Mean absolute deviation
Test time is the time between the first and last AE event

linear scale) distribution for all the tested beams are given in Table 2. The mean absolute deviation given in Table 2 is a robust measure of dispersion in the presence of extreme events. The significant difference between mean absolute deviation and standard deviation indicates the deviation of inter-event time distribution from normality. Figure 2(a) shows the loading history and the AE events over the test duration. One can simply estimate the average rate of AE events occurrence (No. of events/unit time=1/mean(τ) or Time of test/No. of events) from the statistics which increases with respect to size. However, Figure 2(b) shows the comparison between the average event rate and instantaneous event rate determined by averaging over 10 seconds non-overlapping window for a large beam (B2). As mentioned earlier, AE in concrete is a non-Poissonian process exhibiting time-dependent instantaneous event rate occurrence as shown in Figure 2(b). The instantaneous event rate rises and peaks around 500 seconds indicating the clustering of events which then gradually decreases till the end. The instantaneous event rate obviously depends on the loading rate, crack extent, and size of the specimen.

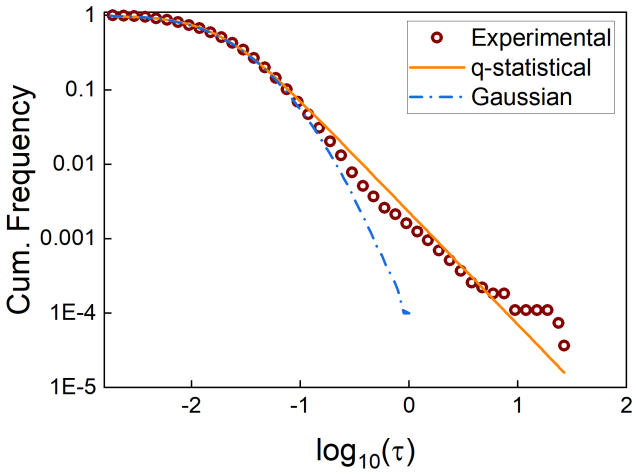

Figure 4: Cumulative distribution on log scale comparing q-statistical and Gaussian distribution fit on experimental data.

5.2 q-STATISTICAL PARAMETERS

The inter-event time distribution for a large-sized beam (B2) is shown in Figure 3. The scale of the inter-event time ranges in order from 10^{-3} to 10^{1} seconds therefore, the logarithmic scale is inevitable for the analysis. Unlike exponential distribution, the inter-event time distribution of AE events on a logarithmic scale shows a right-tailed bell-like curve or skewed Gaussian-like distribution. Figure 4 shows the cumulative frequency distribution of inter-event time distribution fitted with Equation 6 along with the Gaussian distribution. We do not intend to elaborate on the shortfalls of

the Gaussian distribution for modeling the long-tailedness, rather the Gaussian distribution is preferred for comparison due to two reasons. First of all, the right-skewed exponential distribution, mostly linked to waiting time distributions, is inappropriate to compare with the bell-like experimentally observed distribution. Secondarily, Gaussian distribution has an exponentially decaying tail by which we intend to illustrate the relative difference between the tails of Gaussian distribution and observed inter-event time distribution. The NESM-based cumulative distribution function fits well with the experimental data by appropriately modeling the long-tailed behavior.

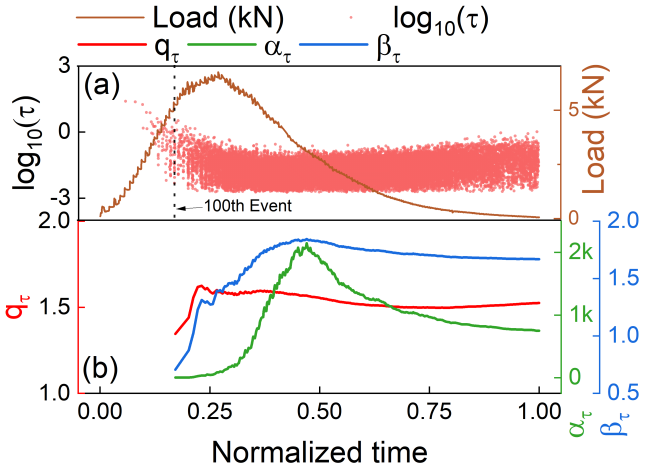

Figure 5: a) Variation of applied load and inter-event time over test time, b) Evolution of q-statistical parameters over time

Figure 5 shows the evolution of q-statistical parameters for a large-sized beam (B2). The scatter plot in Figure 5(a) shows waiting time ($log_{10}\tau$) associated with the AE events for the test duration. In Figure 5(b), the entropic index q_τ increases during the initial phase of AE activity and decreases slightly before approaching a constant value signifying the probability in the distribution tail is constant. Similarly, the location parameter α_τ increases and decreases over time indicating the change in the rate of AE events. The scale parameter β_τ too approaches a constant value after rising steadily indicating convergence of the distribution shape. Comparison of these parameters across the specimen size at failure is shown in Figures 6 and 7. The entropic index q_τ shows a slight increase with the increase in beam size as shown in Figure 6 however, the variation in q_τ is in a small range near $q_\tau \approx 1.5$. The strong size effect is present in the parameters α_τ and β_τ as evident from Figure 7.

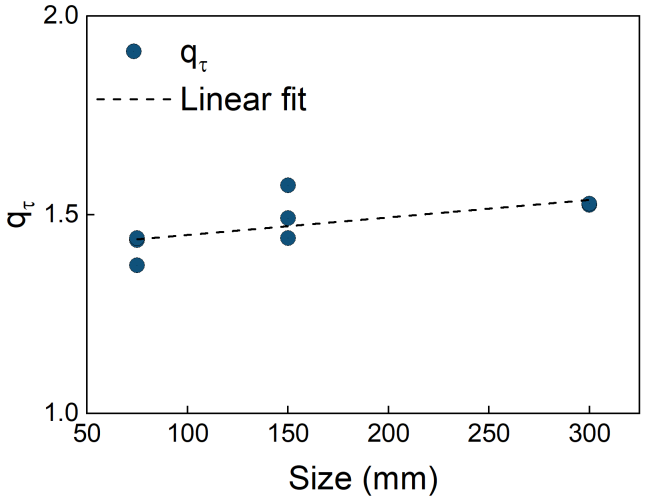

Figure 6: Size dependence of q_τ parameters.

6 DISCUSSION

6.1 PHYSICAL MEANING

The inter-event time distribution, as shown in Figure 3, can be divided roughly into the body and tail parts. The distribution body refers to the central part where the majority of the probability mass is concentrated. The q-statistical framework defines the shape of the evolving inter-event time distribution by apprehending the body and tail part coherently. The entropic index q_τ defines the probability mass in the tail region. Similarly, the bell-like distribution body can be described by α_τ and β_τ as location and scale parameters. The location parameter indicates the central tendency of the distribution while scale parameters characterize the dispersion in the distribution shape (For example, the shape of the Gaussian distribution can be defined by the mean as a location parameter and the standard deviation as a scale parameter). Characterization of the distribution tail region by assigning a separate index q_τ is a pivotal

contribution of the NESM formulation. Most of the frequent AE activity is captured by the distribution body which can be considered as background activity. The extreme events occurring in the tail region, which are not frequent, play a crucial role in the failure process. Higher inter-event time signifies a period of AE quiescence where the time is consumed to accumulate the stress either to sudden release or after suddenly releasing it. Therefore, the entropic parameter q_τ is significant for damage detection.

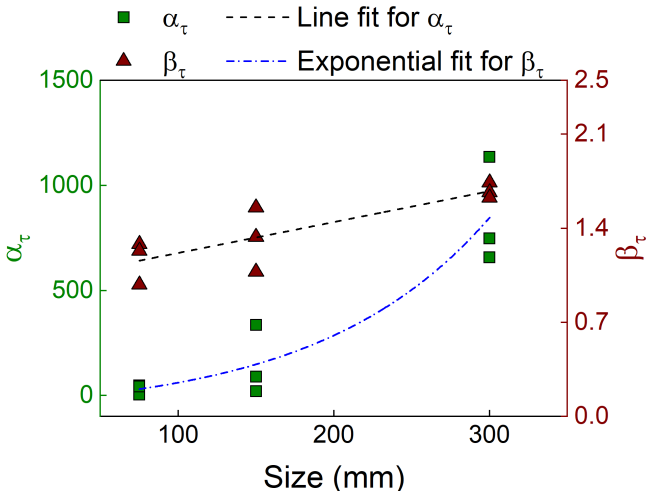

Figure 7: Size dependence of α_τ and β_τ parameters

6.2 COMPARISON WITH MAGNITUDE ENTROPIC INDEX q_m

Despite the randomness of AE inter-event time, the entropic parameter q_τ clusters around $q_\tau \approx 1.5$ for the three beam sizes while the parameters α_τ and β_τ captures size dependence of the distribution. Similar q-statistical parameters for the AE magnitude distribution of the same experiment were determined using power law ansatz-based NESM formulation and reported in [11]. As the present work extends NESM formulation to inter-event time distribution, for the integrity of the work, we discuss the collective behavior of entropic index q_m determined for magnitude distribution and associated entropic index q_τ. The relation between entropic index q_m and q_τ is shown in Figure 8. The entropic index q_m relates with the b-value determined by the Gutenberg-Richter law by the relation $b = \frac{(2-q_m)}{(1-q_m)}$. The universality of b-value $b \approx 1$ at failure is well known in the literature which indicates possible universality of entropic index $q_m \approx 1.5$. Interestingly, the clustering of $q_\tau \approx 1.5$ might also indicate the possible critical value of q_τ for a given loading rate. Consequently, we propose a hypothetical duality relation $q_m + q_\tau \approx 3$. The relationship results in a possible critical line for entropic indices as shown in Figure 8. Such hypothetical duality relationship between inter-event time and distance has been proposed in [13, 14] for exhibiting collective spatio-temporal behavior of earthquakes. Figure 9 shows the variation of $q_m + q_\tau$ with respect to the beam sizes which does not exhibit any size dependence. The relationship is, although speculative and lacks mathematical rigor, experimentally observed and needs further investigation. Moreover, the existence of such a relationship at critical loading may benefit the understanding and damage evaluation in non-critical type load applications such as dynamic, fatigue, and creep.

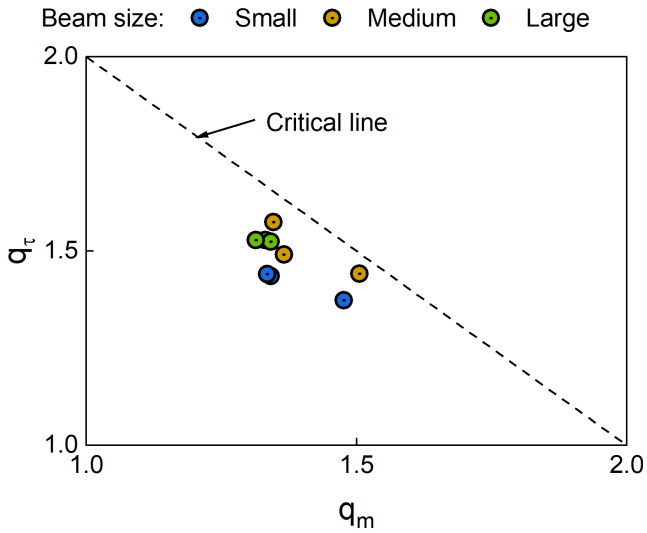

Figure 8: The relation between entropic indices q_τ and q_m. The dashed line represents a possible critical line obtained from the hypothetical relation $q_m + q_\tau \approx 3$.

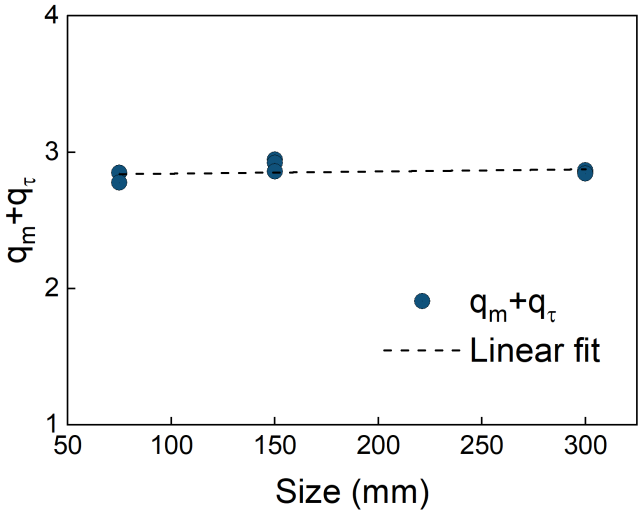

Figure 9: Size dependence of $q_m + q_\tau$

7 CONCLUSIONS

The present work extended NESM formulation to the acoustic emission inter-event time distribution observed during quasi-static loading of concrete beams under three-point bending. The exponential ansatz-based formulation appropriately models the evolving inter-event time distribution resulting in the entropic parameter q_τ and two distribution parameters α_τ and β_τ. The collective behavior of entropic indices q_m and q_τ obtained from the AE inter-event time and magnitude distribution respectively are also discussed in brief. A hypothetical relation $q_m + q_\tau \approx 3$ obtained from the experimental data is an important contribution of the present work. The present work focused on monotonically increasing quasi-static loading which was controlled by crack mouth opening displacement resulting in the variation of the inter-event time along a fixed band. However, in the case of fatigue loading, the variation in the inter-event time will be more erratic as fatigue failure is highly uncertain with significant scatter. The ability of NESM formulation to model such distribution will be addressed in the future.

REFERENCES

[1] Burud, N. & Chandra Kishen, J. M. Application of generalized logistic equation for b-value analysis in fracture of plain concrete beams under flexure. *Engineering Fracture Mechanics*. **210** pp. 228-246 (2019)

[2] Ohno, K. & Ohtsu, M. Crack classification in concrete based on acoustic emission. *Construction And Building Materials*. **24**, 2339-2346 (2010)

[3] Carpinteri, A., Lacidogna, G., Niccolini, G. & Puzzi, S. Critical defect size distributions in concrete structures detected by the acoustic emission technique. *Meccanica*. **43** pp. 349-363 (2008)

[4] Tsallis, C. Possible generalization of Boltzmann-Gibbs statistics. *Journal Of Statistical Physics*. **52** pp. 479-487 (1988)

[5] Vallianatos, F., Papadakis, G. & Michas, G. Generalized statistical mechanics approaches to earthquakes and tectonics. *Proceedings Of The Royal Society A: Mathematical, Physical And Engineering Sciences*. **472**, 20160497 (2016)

[6] Omori, F. On the after-shocks of earthquakes. (The University of Tokyo,1895)

[7] Utsu, T. A statistical study on the occurrence of aftershocks. *Geophys. Mag.*. **30** pp. 521-605 (1961)

[8] Corral, Á. Long-term clustering, scaling, and universality in the temporal occurrence of earthquakes. *Physical Review Letters*. **92**, 108501 (2004)

[9] Saltas, V., Vallianatos, F., Triantis, D., Koumoudeli, T. & Stavrakas, I. Non-extensive statistical analysis of acoustic emissions series recorded during the uniaxial compression of brittle rocks. *Physica A: Statistical Mechanics And Its Applications*. **528** pp. 121498 (2019)

[10] Greco, A., Tsallis, C., Rapisarda, A., Pluchino, A., Fichera, G. & Contrafatto, L. Acoustic emissions in compression of building materials: Q-statistics enables

the anticipation of the breakdown point. *The European Physical Journal Special Topics*. **229** pp. 841-849 (2020)

[11] Burud, N. & Chandra Kishen, J. M. Non-extensive statistical mechanics for acoustic emission in disordered media: Entropy, size effect, and self-organization. *International Journal Of Mechanical Sciences*. **202** pp. 106514 (2021)

[12] Silva, R., França, G., Vilar, C. & Alcaniz, J. Nonextensive models for earthquakes. *Physical Review E*. **73**, 026102 (2006)

[13] Abe, S. & Suzuki, N. Law for the distance between successive earthquakes. *Journal Of Geophysical Research: Solid Earth*. **108** (2003)

[14] Vallianatos, F., Michas, G., Papadakis, G. & Sammonds, P. A non-extensive statistical physics view to the spatiotemporal properties of the June 1995, Aigion earthquake (M6. 2) aftershock sequence (West Corinth rift, Greece). *Acta Geophysica*. **60** pp. 758-768 (2012)